Solubility of chromium oxide in binary soda-silicate melts

H. Khedim, R. Podor, Pierre-Jean Panteix, C. Rapin, Michel Vilasi

Solubility of chromium oxide in binary soda silicate melts

H. Khedim[1], R.Podor[2], P.J. Panteix[1], C. Rapin[1], M.Vilasi[1]

1 Institut Jean Lamour UMR 7198 – Département CP2S – Equipe 206

Faculté des Sciences et Techniques – Nancy Université

Boulevard des Aiguillettes

B.P. 70239 - 54506 VANDOEUVRE les NANCY cedex ; France

2 Institut de Chimie Séparative de Marcoule

UMR 5257 - ICSM Site de Marcoule

B.P. 17171 -30207 BAGNOLS SUR CEZE cedex, France

Abstract

The total chromium oxide (Cr_2O_3) solubility is measured in the liquids belonging to the Na_2O-SiO_2 system using a thermochemical reactor which allows the independent control of temperature (1125°C<T<1250°C), glass composition (1.5<x<3) and oxygen fugacity (-15<log fO_2<-0.61). The contribution of each chromium species (Cr(II), Cr(III) and Cr(VI)) and the total Cr content dissolved in the melt are determined using a model describing the chromium chemistry in melts involving dissolution, redox and oxo-complex reactions. A manipulation of the obtained results allows the determination of physicochemical properties of chromium species in melts (chromium complexes formulas) as well as thermodynamic properties (entropies and enthalpies) related to the dissolution, reduction and oxidation processes of chromium oxide in binary melts.

PACS: 61.43.Fs; 64.75.Bc; 65.20.Jk; 91.67.De; 82.60.Hc

1. Introduction

Chromium can exist under various oxidation states depending on environmental conditions. It is often used in metallurgy as an alloying element due to its hardening and corrosion resistance properties. In the glass industry, most of the equipments are made up of superalloys containing up to 30% of chromium. The lifetime of metallic parts, which are in contact with molten glasses, is mainly controlled by high temperature corrosion, and the degradation of the alloys or superalloys immersed in the molten glasses is governed by dissolution and oxido-reduction reactions [1-4]. The corrosion resistance is conditioned by the formation of a protective layer of chromium oxide at the metal/glass interface. As a consequence, the knowledge of chromium oxide dissolution in simple silicate melts will provide useful information concerning the understanding of the ability of these alloys to resist against glass melts corrosion.

Several studies have been dedicated to the chromium oxide dissolution process in silicate melts [4-11]. The first type of studies deal with corrosion reaction of chromium containing alloys [4,5]. Other studies report the dissolution of chromium oxides in glass melts [6-11]. The authors have demonstrated that the solubility of chromium oxide strongly depends on glass basicity (melt composition), temperature and oxygen fugacity [6-8,12]. This latter parameter influences the redox properties of the glass and yields to the stabilization of high or low oxidation states of the multivalent elements in the melt. Therefore the effects related to the action of both O^{2-} (basicity effect) and O_2 (redox effect) rule together the chromium chemistry in silicate melts, as described by Tilquin et al [10]. Oxygen is one of the principal reactants in redox equilibria occuring in molten glasses [13,14]. The equilibrium state of the medium strongly depends on its composition, which fixes the O^{2-} activity (i.e. for a given basicity). Thus, for glasses of fixed O^{2-} activity, the measurement of dissolved oxygen can be

used to control some processes, such as the melt properties (viscosity, quality of refining) or the final state of the material (colour, ageing…) [15-18].

Regarding the behavior of Cr_2O_3 in molten glasses, the various interactions occurring between the silicate melt and chromia are presented in previous works [6,8-11] and the related chemical reactions are described hereafter:

$$\frac{1}{2}Cr_2O_3(crystal) \Leftrightarrow Cr(III)O_x^{(2x-3)-}(melt) + \left(\frac{3}{2} - x\right)O^{2-}(melt) \qquad \text{Eq. 1}$$

Cr(III) species can be oxidized into Cr(VI) species (Eq. 2), under oxidizing conditions, or reduced to Cr(II) species (Eq. 3), under reducing conditions:

$$Cr(III)O_x^{(2x-3)-}(melt) + \frac{3}{4}O_2(gas) \Leftrightarrow Cr(VI)O_y^{(2y-6)-}(melt) + \left(x - y + \frac{3}{2}\right)O^{2-}(melt) \qquad \text{Eq. 2}$$

$$Cr(III)O_x^{(2x-3)-}(melt) + \left(z - x + \frac{1}{2}\right)O^{2-}(melt) \Leftrightarrow Cr(II)O_z^{(2z-2)-}(melt) + \frac{1}{4}O_2(gas) \qquad \text{Eq. 3}$$

The equilibrium constants for the dissolution, oxidation, and reduction reactions can be expressed as:

$$K_{diss} = a[O^{2-}]^{\left(\frac{3}{2}-x\right)}.a[Cr(III)] \qquad \text{Eq. 4}$$

$$\log[Cr(III)] = \log K_{diss} + \left(x - \frac{3}{2}\right)\log a(O^{2-}) \qquad \text{Eq. 5}$$

$$K_{ox} = \frac{a[Cr(VI)].a[O^{2-}]^{\left(x-y+\frac{3}{2}\right)}}{a[Cr(III)].fO_2^{3/4}} \qquad \text{Eq. 6}$$

$$\log\frac{[Cr(VI)]}{[Cr(III)]} = \frac{3}{4}\log fO_2 - \left(x - y + \frac{3}{2}\right)\log a[O^{2-}] + \log K_{ox} \qquad \text{Eq. 7}$$

$$K_{red} = \frac{a[Cr(II)].fO_2^{1/4}}{a[Cr(III)].a[O^{2-}]^{(z-x+\frac{1}{2})}} \qquad \text{Eq. 8}$$

$$\log\frac{[Cr(II)]}{[Cr(III)]} = -\frac{1}{4}\log fO_2 + \left(z - x + \frac{1}{2}\right)\log a[O^{2-}] + \log K_{red} \qquad \text{Eq. 9}$$

Where $a_i = \gamma_i.X_i$

With a_i is the activity, γ_i the activity coefficient and X_i the molar fraction of species i.

In glass melts, polyvalent ions contents are generally very low. Consequently, their concentrations are also very low. Therefore, in conformity with Henry's law, the activity can be assimilated to the concentration.

The model developed in our previous works [5,6] allowed the determination of the redox ratio (Cr(II)/Cr(III) and Cr(VI)/Cr(III)), the chromium complexes formulas and the thermodynamic data concerning the reactions occurring in the Na_2O-$3SiO_2$ melt composition. The aim of this work is to determine the chromium speciation (Cr(II), Cr(III) and Cr(VI) contents and their ratios) in the Na_2O-SiO_2 system by taking into account the model developed in a previous work [6]. The expected results should allow the determination of the chromium complexes formulas (x, y and z parameters) and thermodynamic data related to the dissolution, oxidation and reductions processes.

2. Experimental

Soda-silicate glasses with the general composition of Na_2O- $xSiO_2$ (x=1.5, 2, 2.5 and 3) were synthetised from reagent grade SiO_2 (Chempur 99.9 %) and Na_2CO_3 (Chempur 99.5%). Appropriate amounts of the reagent powders were weighed and mixed, then introduced in a $Pt_{95}Au_5$ crucible and heated in a muffle furnace. In order to minimise the sodium loss by volatilisation [19,20], not less than 200 grams of glass were melted and the thermal cycle was defined as follows: 1200°C for 2h, 1400°C for 2h and then 1100°C for 24h. The melts were then quenched and finally crushed. Glass compositions were systematically checked by electron probe microanalysis: the aimed and obtained glass compositions are reported in Table 1.

Ten grams of each resulting glass composition were mixed to 5 wt.% Cr_2O_3, finely ground and melted at 1200°C for 5 minutes in a platinum crucible. The process was performed three

times in order to ensure a regular distribution of the Cr_2O_3 grains in the glass network. The required quantity of glass mixed with Cr_2O_3 (about 100 mg) was taken from the mixture, put in a carbon crucible, heated at 1200 °C for 1 minute and finally quenched in air. Due to the high surface tension between the melt and the carbon crucible, the sample forms a perfect glass ball.

Alkali elements volatilise easily from silicate melts at high temperature [21]. The rate of sodium volatilisation increases with increasing temperature and alkali content, and decreases with increasing fO_2 and sample size [22]. This can lead to drastic changes in the melt composition during long term experiments. In order to avoid volatilisation, the experiments were performed in a closed system using a method developed in the laboratory [6,23]. It allows the independent control of oxygen fugacity, temperature and alkali activity in the silicate melt.

The experiment principle is as described in previous works [5,6,23]: the cell is constituted by a sealed silica tube of around 25–30 cm^3 ($Ø^{ext}$ = 22 mm, h ≈ 120 mm) containing several components that impose the thermochemical parameters of the system. The studied glass balls (samples) were mounted on a platinum lid by using a platinum wire. In order to limit the Na_2O volatilisation from the sample, the Na partial vapour pressure was imposed to the sample by adding a platinum crucible ($Ø^{ext}$ = 18 mm, h = 20 mm) containing 5 g of glass (source) which has the same composition with the sample. Assuming that the reference melt quantity in the reactor is large enough as compared to the molten samples, this device will ensure that, at thermodynamic equilibrium, the $aNaO_{1/2}$ in the sample will be the same than in the reference melt according to the following reactions:

$$NaO_{1/2}^{(\text{reference melt})} \rightarrow Na_{(g)} + 1/4\ O_2 \qquad \text{Eq. 10}$$

$$Na_{(g)} + 1/4\ O_2 \rightarrow NaO_{1/2}^{(sample)} \quad \text{Eq. 11}$$

$$aNaO_{1/2}^{(sample)} = aNaO_{1/2}^{(reference\ melt)} \quad \text{Eq. 12}$$

The oxygen fugacity in the device is controlled by a solid M/M_xO_y buffer (M = Metallic element; Fe/FeO, FeO/Fe_3O_4, Co/CoO, Ni/NiO and Fe_3O_4/Fe_2O_3) incorporated below the reference reservoir either at the bottom of the silica tube or in an alumina crucible in order to prevent reactions with the silica tube and to avoid alloying between the solid buffer and the platinum crucible. The silica tube was then evacuated and directly sealed under secondary vacuum. Direct measurements show that the residual pressures inside the thermochemical cell never exceed 10^{-6} bar at room temperature.

The silica tubes were introduced in a muffle furnace directly at the experimental temperature on an alumina support for a vertical maintain of the cell.

After the adequate heat treatment [24], the silica tubes were removed from the furnace and directly quenched into water. The cooling rate is estimated to be 50°C/s for the first 10s of the quenching. Each part of the reactor was weighed before and after experiment in order to look for potential leaks. Special attention, by careful observation and analyses, was paid onto the $Na_2O–xSiO_2$ melt reservoir and the melt drop holder. Finally, the presence of both metal and oxide phases in the solid buffer after each run was checked by optical microscope and X-ray diffraction.

The glass compositions as well as the total amount of dissolved chromium in melts were determined using a CAMECA SX100 electron microprobe at the Université Henri Poincaré, Nancy-Université (France). The main difficulty, when analysing glasses with high Na contents is to determine the sodium content with accuracy and with limited sodium volatilisation during measurement. The optimised conditions for the analysis of homogeneous glasses are an acceleration voltage of 25 kV, a beam intensity of 8 nA, an electron beam size

of 10 μm. The counting times on peaks and backgrounds are (6 s, 3 s), (10 s, 5 s) and (30s, 15) respectively for Na, Si and Cr. Each element was analysed with a specific spectrometer allowing the quantification of the three elements at once. However, this also allows the limitation of both analysis duration as well as Na_2O volatilisation. Each glass composition and total chromium content were determined by a mean of 15–20 individual analyses. The standards which were used in these analyses are Cr_2O_3 for Cr and $NaAlSi_3O_8$ for Na and Si. The oxygen content was determined by stoechiometry associating the oxidation numbers I, IV and III for Na, Si and Cr, respectively.

The presence of excess chromia crystallites in the sample was systematically checked by electron backscattered imaging (Figure 1). In order to measure the dissolved chromium species with accuracy, the analysed zone was chosen in the vicinity of remaining Cr_2O_3 crystallites. Not less than 25 to 30 microprobe analyses were performed on each sample. The results were averaged and the standard deviation was calculated: the extreme data, which are too far from the mean value, were rejected and the procedure was repeated. The data used in this work are the mean values determined from 10 measurements performed by following this procedure. The standard deviations have been considered as the error bars. They are always in the range of 5% from the mean value. This proves that there is no local segregation of Cr_2O_3 crystals and that the analysed samples have reached their equilibrium state.

3. Results

Only equilibrium values were taken into account. The minimum run duration necessary to reach the equilibrium state was determined by performing a preliminary kinetic investigation [24]: in most cases, it was about 2 hours. The chromium solubility in molten silicates was

studied as a function of temperature, oxygen fugacity and glass composition. All the obtained results are summarised in Table 2.

The total chromium content in the melt was plotted as a function of oxygen fugacity for different glass compositions (Figure 2). It can be concluded that the chromium content variations with melt composition follow the same phenomenon for any values of temperature:

- Under an oxidizing atmosphere, the solubility increases with the basicity (alkaline oxides content) of glass.
- Under a reducing atmosphere, the solubility decreases when the basicity increases.

The total chromium content was also plotted as a function of oxygen fugacity for different temperatures for a given glass composition (N2S) in Figure 3. It can be concluded that the total chromium content in the melt increases with temperature for any values of oxygen fugacity.

Independently of the temperature or the glass composition, the general shape of the obtained curves remains unchanged. It always comprises three distinct fields of solubility which are characteristic of the presence of the three chromium valences (Cr(II), Cr(III) and Cr(VI)) [6].

4. Discussion

The speciation of the chromium species has been determined using the same model as that proposed in previous works [5,6] : when the equilibrium is reached, the total chromium dissolved in the glass Cr(tot) is considered as the sum of all chromium species:

$$Cr(tot) = Cr(II) + Cr(III) + Cr(VI) \qquad \text{Eq. 13}$$

Using the same assumption, for a given temperature, we consider that the Cr(III) species dissolved in the melt which is in equilibrium with solid Cr_2O_3 crystallites, remains constant for any value of oxygen fugacity [6,11]. This assumption is convinced by the fact that chromium oxide dissolution (Eq. 1) is an acid-base reaction which does not depend on oxygen fugacity. The minimum value of chromium content in the glass corresponds to the Cr(III) contribution. Therefore, under oxidizing conditions, Cr(II) content can be neglected as compared to Cr(III) and Cr(VI). In the same way, under reducing conditions, Cr(VI) can be neglected as compared to Cr(III) and Cr(II). With these considerations, it can be simplified as the following equations:

Under oxidizing conditions

$$Cr(tot) = Cr(III) + Cr(VI) \qquad \text{Eq. 14}$$

Under reducing conditions

$$Cr(tot) = Cr(II) + Cr(III) \qquad \text{Eq. 15}$$

Chromium speciation could be determined by considering these assumptions. Thus the redox ratios, defined as R_{ox}=Cr(VI)/Cr(III) and R_{red} =Cr(II)/Cr(III), can be calculated. In order to confirm or reinforce the proposed model, the plots of the redox ratio values as a function of $\log fO_2$ are performed. In fact, Eq. 7 and Eq. 9 show that, for a given melt composition and temperature, the logarithm of the redox ratio varies linearly with oxygen fugacity and the slope value is equal to -0.25 under reducing conditions and 0.75 under oxidizing conditions. Logarithms of the obtained redox ratios in the Na_2O-$2SiO_2$ glass composition have been plotted as a function of $\log fO_2$ for different temperatures (Figure 4): the correlation between both parameters is linear with slope values thus in perfect agreement with the theoretical values. This behavior is observed for each temperature of the studied temperature range. Redox ratios values being given and confirmed and the complex formulas of the various

chromium species formed in molten glass can be determined by plotting the logarithms of Cr(III), R_{ox} and R_{red} values, for a given temperature and oxygen fugacity, as a function of $a(O^{2-})$ of the melt. The variations should be linear. The x, y and z parameters relative to each chromium complex ($Cr(II)O_z^{(2z-2)-}$, $Cr(III)O_x^{(2x-3)-}$ and $Cr(VI)O_y^{(2y-6)-}$) can be thus deduced from the slope values of the obtained lines (*x-1.5*, *y-x-1.5* and *z-x+0.5*) in agreement with Eq. 5, 7 and 9 respectively.

First of all, a reliable data set concerning the O^{2-} activities should be available. In the case of the Na_2O-SiO_2 binary melts, the O^{2-} activity can be assimilated to the Na_2O activity [25-27]. The values of Na_2O activities (in the Na_2O-SiO_2 system) that are in the literature are strongly dispersed. Therefore, we decided to select the most recent data set that was published by Abdelouhab *et al.* [28,29]. Logarithms of Cr(III), R_{ox} and R_{red} values were plotted as a function of $\log[a(O^{2-})]$ for different temperatures, and for a given fO_2 : examples of these kinds of plots are given in Figure 5. As expected, the variations are linear. The obtained slope values, the calculated x, y and z parameters as well as the chromium complexes formulas are summarized in Table 3. The slope values presented here are the average values of the slopes determined experimentally for the different fO_2. The error bars correspond to the standard deviations of the experimental slopes.

These parameters are extrapolated after multiple processing of experimental data, and it should be noted that the x, y and z values remain constant with the temperature (Figure 6), even if the slope values differ from one temperature to another. Consequently, important information has to be highlighted: only one complex, for each oxidation state of chromium, can exist in the studied range of temperature. At this stage, the compositions suggested for the chromium species are Cr_2O^{2+}, $Cr_3O_4^{+}$ and $Cr_2O_7^{2-}$ for Cr(II), Cr(III) and Cr(VI) respectively.

Tilquin *et al.* [10], who studied chromium oxide dissolution in soda silicate melts, have determined that (y-x) is equal to 2,88 (≈ 3) and suggested that the composition of the Cr(VI)

complex is CrO_4^{2-}. Consequently, the composition suggested for the chromium complex containing Cr(III) is CrO^+. This is not in agreement with the compositions of the complexes obtained in this work. This difference can be explained by the fact that Tilquin *et al.* [10] have performed their study at T=1000°C while the temperature domain explored during this work rises from 1125 to 1350°C. Indeed, the chromium complex compositions can drastically change with melting temperature.

As it has just been shown, x, y and z parameters are constant in the range of temperatures studied here (Figure 6). Consequently, it is possible to carry out calculations allowing the determination of thermodynamic data (standard enthalpies and entropies) relative to the dissolution, oxidation and reduction reactions [6] of chromia for the various Na_2O-SiO_2 melt compositions. The thermodynamic development is as follows:

For given oxygen fugacity and glass composition, Eq. 5, 7 and 9 can be written:

$$\log[Cr(III)] = A \qquad \text{Eq. 16}$$

$$\log\frac{[Cr(VI)]}{[Cr(III)]} = \frac{3}{4}\log fO_2 + B \qquad \text{Eq. 17}$$

$$\log\frac{[Cr(II)]}{[Cr(III)]} = -\frac{1}{4}\log fO_2 + C \qquad \text{Eq. 18}$$

with

$$A = \log K_{diss} + \left(x - \frac{3}{2}\right)\log a[O^{2-}] \qquad \text{Eq. 19}$$

$$B = \log K_{ox} - \left(x - y + \frac{3}{2}\right)\log a[O^{2-}] \qquad \text{Eq. 20}$$

$$C = \log K_{red} + \left(z - x + \frac{1}{2} \right) \log a[O^{2-}] \quad \text{Eq. 21}$$

By plotting log[Cr(III)] as a function of (1/T) for a given glass composition, we notice that the behavior follows an Arrhenius law (Figure 7) and can be written:

$$\log[Cr(III)] = A' + \frac{A''}{T} \quad \text{Eq. 22}$$

Equilibrium constant, as well as O^{2-}, activity depends on temperature as shown by the following equations:

$$\log K = -\frac{\Delta H^0}{2.3R}\left(\frac{1}{T}\right) + \frac{\Delta S^0}{2.3R} \quad \text{Eq. 23}$$

$$\log[a(O^{2-})] = \alpha + \frac{\beta}{T} \quad \text{Eq. 24}$$

As it has been mentioned before, O^{2-} activity is comparable to Na_2O activity. α and β parameters are well known for the Na_2O-SiO_2 system [28]. By replacing the K_{diss} and aO^{2-} with their respective expressions, log[Cr(III)] as a function of (1/T) can be divided into entropic and enthalpic terms:

$$\log[Cr(III)] = \left[\frac{\Delta S^0}{2.3R} - \left(x - \frac{3}{2} \right)\alpha \right] + \left[\frac{-\frac{\Delta H^0}{2.3R} - \left(x - \frac{3}{2} \right)\beta}{T} \right] \quad \text{Eq. 25}$$

With

$$\left[\frac{\Delta S^0}{2.3R} - \left(x - \frac{3}{2} \right)\alpha \right] = A' \text{ and } \left[-\frac{\Delta H^0}{2.3R} - \left(x - \frac{3}{2} \right)\beta \right] = A''$$

At this step, standard enthalpy and entropy of chromium dissolution process can be expressed, for a glass composition, as a function of the determined parameters:

$$\Delta S^{0}_{diss} = 2.3R\left[A' + \left(x - \frac{3}{2} \right)\alpha \right] \quad \text{Eq. 26}$$

$$\Delta H^{0}_{diss} = 2.3R\left[-A'' - \left(x - \frac{3}{2} \right)\beta \right] \quad \text{Eq. 27}$$

B and C parameters (Eq. 16 and Eq. 17) correspond to the Y-axis intercept when plotting log[Cr(VI)/Cr(III)] and log [Cr(II)/Cr(III)] respectively as a function of logfO_2 (Figure 4). The evolution of this two parameters (B and C) as a function of reverse temperature (1/T), for a given glass composition, is linear (Figure 8) and follows an Arrhenius law as :

$$B = B' + \frac{B''}{T} \quad \text{Eq. 28}$$

$$C = C' + \frac{C''}{T} \quad \text{Eq. 29}$$

Considering B and C expressions (Eq. 17 and Eq. 18), and by replacing $\log K_{ox}$, $\log K_{red}$ and log aO^{2-} (Eq. 20 and Eq. 21) by their respective expressions, B and C parameters can be written as:

$$B = \left[\left(y - x - \frac{3}{2} \right)\alpha + \frac{\Delta S^{0}_{ox}}{2.3R} \right] + \frac{\left(y - x - \frac{3}{2} \right)\beta - \frac{\Delta H^{0}_{ox}}{2.3R}}{T} \quad \text{Eq. 30}$$

$$C = \left[\left(z - x + \frac{1}{2} \right)\alpha + \frac{\Delta S^{0}_{red}}{2.3R} \right] + \frac{\left(z - x + \frac{1}{2} \right)\beta - \frac{\Delta H^{0}_{red}}{2.3R}}{T} \quad \text{Eq. 31}$$

Standard enthalpies and entropies of oxidation and reduction reactions can thus be determined by identification and expressed as follows:

$$\Delta S_{ox}^{0} = 2.3R\left[B' - \left(y - x - \frac{3}{2} \right)\alpha \right] \quad \text{Eq. 32}$$

$$\Delta H_{ox}^{0} = 2.3R\left[\left(y - x - \frac{3}{2} \right)\beta - B'' \right] \quad \text{Eq. 33}$$

$$\Delta S_{red}^{0} = 2.3R\left[C' - \left(z - x + \frac{1}{2} \right)\alpha \right] \quad \text{Eq. 34}$$

$$\Delta H_{red}^{0} = 2.3R\left[\left(z - x + \frac{1}{2} \right)\beta - C'' \right] \quad \text{Eq. 35}$$

Standard entropies and enthalpies for chromium dissolution, reduction and oxidation in the Na_2O-SiO_2 system, obtained by the thermochemical calculations, are reported in Table 4.

Considering the set of data related to the dissolution process, $\Delta H°_{diss}$ and $\Delta S°_{diss}$ values, given for the whole Na_2O-SiO_2 composition range, are homogeneous around a median value of 85 ± 5 kJ.mol^{-1}and 22 ± 5 J.mol^{-1}.K^{-1} respectively. Moreover, if we compare $\Delta H°_{diss}$ values, calculated in this study, with those measured by Kim *et al.* [30] in borosilicate systems it comes that all these values are coherent. This justifies *a posteriori* the chosen approach.

5. Conclusion

Several important features of the chromium chemistry in silicate melts were drawn up in this study. Among those, it is advisable to recall that:

- The development of an original experimental device allowed the determination of the Cr_2O_3 solubility limits in the Na_2O-$xSiO_2$ system as a function of experimental parameters.
- The chromium species speciation and thus the redox ratios could be determined by using a relatively simple model.
- The influence of the experimental parameters (temperature, oxygen fugacity and glass composition) on the redox ratio has been evidenced. In fact, it has been shown that an increase in the temperature leads to an increase in the redox ratio and that basicity of the melt stabilises the oxidised forms.
- The unicity of the complex compositions, associated to the various chromium valences, in the studied range of temperature and glass composition (Na_2O-SiO_2 system) have been proved.
- Chromium complexes compositions $Cr_2O_7^{2-}$, $Cr_3O_4^{+}$ and Cr_2O^{2+} are proposed for Cr(II), Cr(III) and Cr(VI) species respectively.
- The thermodynamic data related to the dissolution, the reduction and the oxidation processes of chromium oxide in the soda-silicate system could be determined.

A complete set of data, concerning the chromium solubility limits in the Na_2O-SiO_2 system is proposed as a function of temperature, glass composition and oxygen fugacity. A recent work [31] presents a similar approach in calcium silicate base melts, with a phenomenology in good agreement with ours. Nevertheless, further studies have been performed here: oxo-complexes formulas, thermodynamic data and evolution of redox with melt basicity have been proposed.

Acknowledgements

The authors are grateful to J. Ravaux and S. Mathieu for performing EPMA (Service Commun d'Analyses par Microsonde Electronique de Nancy). This work was financially supported by the ANR BLAN06-3_134633 through the Actimelt project.

References

[1] J. Di Martino, C. Rapin, P. Berthod, R. Podor, P. Steinmetz, Corros. Sci. 46 (2004) 1849.

[2] J. Di Martino, C. Rapin, P. Berthod, R. Podor, P. Steinmetz, Corros. Sci. 46 (2004) 1865.

[3] A. Carton, C. Rapin, R. Podor, P. Berthod, J. Electrochem. Soc. 153 (2006) B121.

[4] S. Abdelouhab, C. Rapin, R. Podor, P. Berthod, M. Vilasi, J. Electrochem. Soc. 154 (2007) C500.

[5] H. Khedim, Etude de la solubilité de la chromine dans les silicates fondus - Détermination de Grandeurs physicochimiques et Thermodynamiques, PhD Thesis,. Université Henri Poincaré, Nancy (2008).

[6] H. Khedim, R. Podor, C. Rapin, M. Vilasi, J. Am. Ceram. Soc. 91 (2008) 3571.

[7] G. Calas, O. Majerus, L. Galoisy, L. Cormier, Chem. Geol. 229 (2006) 218.

[8] A. J. Berry, H. S. C. O'Neill, D. R. Scott, G. J. Foran, J. M. G. Shelley, Am. Mineral. 91 (2006) 1901.

[9] J. Y. Tilquin, P. Duveiller, J. Glibert, P. Claes, J. Non-Cryst. Solids. 224 (1998) 216.

[10] J. Y. Tilquin, P. Duveiller, J. Glibert, P. Claes, J. Non-Cryst. Solids. 211 (1997) 95.

[11] P. L. Roeder, I. Reynolds, J. Petrol. 32 (1991) 909.

[12] W. Thiemsorn, K. Keowkamnerd, P. Suwannathada, H. Hessenkemper, S. Phanichaphant, B. Mater. Sci. 30 (2007) 487.

[13] M. Roskoz, M.J. Toplis, D.R. Neuville, B.O. Mysen, Am. Mineral. 93 (2008) 1749.

[14] V. Magnien, D.R. Neuville, L. Cormier, J. Roux, J.L. Hazemann, d. de Ligny, S. Pascarelli, I. Vickridge, O. Pinet, P. Richet, Geochim. Cosmichim. Ac. 72 (2008) 2157.

[15] A. Paul, Chemistry of Glasses 2nd Ed., Chapman and Hall, London (1989).

[16] H. Rawson, Properties and Applications of Glass, Elsevier Scientific Pub (1980).

[17] P. Claes, F. Mernier, L. Wery, J. Glibert, Electrochim. Acta. 44 (1999) 3999.

[18] R. H. Doremus, Glass Science, John Wiley and Sons, New York (1994).

[19] L. S. Walter, M. K. Carron, Geochim. Cosmichim. Ac.28 (1964) 937.

[20] J. Konta, L. Mrâz, Mineral. Mag. 40 (1975) 70.

[21] L. S. Walter, J. E. Giutronich, Sol. Energy. 11 (1967) 163.

[22] A. Tsuchiyama, H. Nagahara, I. Kushiro, Geochim. Cosmichim. Ac. 45 (1981) 1357.

[23] R. Mathieu, H. Khedim, G. Libourel, R. Podor, L. Tissandier, E. Deloule, F. Faure, C. Rapin, M. Vilasi, J. Non-Cryst. Solids. 354 (2008) 5079

[24] H. Khedim, S. Abdelouhab, R. Podor, C. Rapin, M. Vilasi, P.J. Panteix, M. J. Toplis, F. Faure, Kinetic Study of the Chromium Solubility in Soda-Silicate Melts, submitted in Journal of Non-Crystalline Solids (2010).

[25] W. Stegmaier, A. Dietzel, Glastech. Ber. 18 (1940) 297.

[26] G. W. Toop, C. S. Samis, Can. Metall. Quart. 1 (1962) 129.

[27] M. Perander, K. H. Karlsson, J. Non-Cryst. Solids. 80 (1986) 387.

[28] S. Abdelouhab, R. Podor, C. Rapin, M. J. Toplis, P. Berthod, M. Vilasi, J. Non-Cryst. Solids. 354 (2008) 3001.

[29] S. Abdelouhab, Détermination de grandeurs physico-chimiques dans les verres fondus - relation avec le comportement à la corrosion du chrome et d'alliages chromine-formeurs, PhD Thesis,. Université Henri Poincaré, Nancy (2005).

[30] C.-W. Kim, K. Choi, J.-K. Park, S.-W. Shin, M.-J. Song, J. Am. Ceram. Soc. 84 (2001) 2987.

[31] A.-M. Mirzayousef-Jadid, K. Schwerdtfeger, Metall. Mater. Tran. B. 40B (2009) 533.

Table 1: Composition of glasses used as starting materials

Aimed glass Composition	**Theoretical Na (at%)**	**Theoretical Si (at%)**	**Na (at.%) WDS**	**Si (at.%) WDS**	**X**
Na_2O–**1.5**SiO_2	26.67	20.00	25.95 (0.40)	20.17 (0.19)	**1.56** (0.04)
Na_2O–**2**SiO_2	22.22	22.22	21.91 (0.44)	22.38 (0.22)	**2.04** (0.06)
Na_2O–**2.5**SiO_2	19.04	23,81	19.22 (0.49)	23.72 (0.25)	**2.47** (0.09)
Na_2O–**3**SiO_2	16.67	25.00	16.34 (0.22)	25.16 (0.11)	**3.08** (0.06)
Na_2O–**3.5**SiO_2	14.81	25.92	14.94 (0.19)	25.86 (0.09)	**3.46** (0.06)

Table 2: *Total content of chromium dissolved in the Na_2O-SiO_2 melts as a function of temperature, glass composition and oxygen fugacity.*

T=1250°C					
Redox buffer	**logfO_2**	**Na_2O-1.5SiO_2**	**Na_2O-2SiO_2**	**Na_2O-2.5SiO_2**	**Na_2O-3SiO_2**
		At.% Cr	**At.% Cr**	**At.% Cr**	**At.% Cr**
Fe/FeO	-11.28	0.437 (0.042)	0.571(0.055)	0.769 (0.070)	1.035 (0.042)
Co/CoO	-8.70	0.308 (0.037)	0.395 (0.021)	0.500 (0.024)	0.619 (0.024)
Ni/NiO	-6.51	0.275 (0.038)	0.359 (0.022)	0.442 (0.005)	0.532 (0.013)
Fe_3O_4/Fe_2O_3	-1.80	0.685 (0.012)	0.685 (0.04)	0.605 (0.031)	0.628 (0.047)
Air	-0.67	3.187 (0.206)	2.755 (0.15)	1.727 (0.218)	1.424 (0.082)
T=1200°C					
Redox buffer	**logfO_2**	**Na_2O-2SiO_2**	**Na_2O-2.5SiO_2**	**Na_2O-3SiO_2**	**Na_2O-3.5SiO_2**
		At.% Cr	**At.% Cr**	**At.% Cr**	**At.% Cr**
Fe/FeO	-11.89	0.581 (0.012)	0.633(0.067)	0.873 (0.047)	1.05 (0.029)
Co/CoO	-9.25	0.349 (0.08)	0.431 (0.017)	0.536 (0.021)	0.510 (0.014)
Ni/NiO	-7.05	0.320 (0.015)	0.389 (0.010)	0.469 (0.010)	0.474 (0.015)
Fe_3O_4/Fe_2O_3	-1.84	0.547 (0.003)	0.518 (0.031)	0.552 (0.024)	0.532 (0.008)
Air	-0.67	2.128 (0.113)	1.492 (0.097)	1.259 (0.058)	0.942 (0.033)
T=1175°C					
Redox buffer	**logfO_2**	**Na_2O-1.5SiO_2**	**Na_2O-2SiO_2**	**Na_2O-2.5SiO_2**	**Na_2O-3SiO_2**
		At.% Cr	**At.% Cr**	**At.% Cr**	**At.% Cr**
Fe/FeO	-12.21	0.295 (0.027)	0.494(0.033)	0.612 (0.027)	0.822 (0.029)
Co/CoO	-9.54	0.225 (0.011)	0.328 (0.009)	0.413 (0.019)	0.498 (0.020)
Ni/NiO	-7.34	0.214 (0.009)	0.290 (0.009)	0.371 (0.028)	0.435 (0.021)
Fe_3O_4/Fe_2O_3	-1.87	0.485 (0.015)	0.481 (0.025)	0.482 (0.024)	0.507 (0.026)
Air	-0.67	2.436 (0.206)	1.834 (0.049)	1.415 (0.034)	1.172 (0.040)
T=1125°C					
Redox buffer	**logfO_2**	**Na_2O-1.5SiO_2**	**Na_2O-2SiO_2**	**Na_2O-2.5SiO_2**	**Na_2O-3SiO_2**
		At.% Cr	**At.% Cr**	**At.% Cr**	**At.% Cr**
Fe/FeO	-12.90	0.223 (0.015)	0.438 (0.011)	0.562 (0.025)	0.768 (0.026)
Co/CoO	-10.14	0.196 (0.029)	0.284 (0.011)	0.388 (0.020)	0.466 (0.026)
Ni/NiO	-7.94	0.191 (0.004)	0.254 (0.004)	0.326 (0.011)	0.379 (0.012)
Fe_3O_4/Fe_2O_3	-1.93	0.395 (0.028)	0.368 (0.007)	0.418 (0.001)	0.436 (0.018)
Air	-0.67	1.980 (0.221)	1.297 (0.084)	1.215 (0.058)	0.990 (0.063)

Table 3: *x, y and z values and chromium complex formulae determined for the different investigated temperatures in the Na_2O-SiO_2 melts*

	T=1250°C	T=1200°C	T=1175°C	T=1125°C	Average values
x-3/2	-0.18 (0.03)	-0.17 (0.04)	-0.15 (0.03)	-0.15 (0.03)	
y-x-3/2	0.73 (0.13)	0.66 (0.14)	0.42 (0.08)	0.40 (0.08)	
z-x+1/2	-0.30 (0.05)	-0.26 (0.05)	-0.24 (0.04)	-0.36 (0.07)	
x	1.35 (0.03)	1.33 (0.04)	1.35 (0.03)	1.35 (0.03)	1.345
y	3.50 (0.16)	3.49 (0.18)	3.27 (0.10)	3.24 (0.11)	3.375
z	0.55 (0.08)	0.57 (0.09)	0.61 (0.08)	0.49 (0.10)	0.555
Cr(III)	$Cr_3O_4^+$	$Cr_3O_4^+$	$Cr_3O_4^+$	$Cr_3O_4^+$	
Cr(VI)	$Cr_2O_7^{2-}$	$Cr_2O_7^{2-}$	$Cr_2O_7^{2-}$	$Cr_2O_7^{2-}$	
Cr(II)	Cr_2O^{2+}	Cr_2O^{2+}	Cr_2O^{2+}	Cr_2O^{2+}	

Table 4: Standard entropies and enthalpies of chromium dissolution, reduction and oxidation reactions in the Na_2O-SiO_2 system

	$\Delta H°_{diss}$ (kJmol^{-1})	$\Delta S°_{diss}$ (JK^{-1}mol^{-1})	$\Delta H°_{oxy}$ (kJ mol^{-1})	$\Delta S°_{oxy}$ (JK^{-1}mol^{-1})	$\Delta H°_{red}$ (kJmol^{-1})	$\Delta S°_{red}$ (JK^{-1}mol^{-1})
Na_2O-1.5SiO_2	85 ± 4	18 ± 5	-105 ± 8	35 ± 5	218 ± 43	49 ± 8
Na_2O-2SiO_2	88 ± 1	24 ± 4	-63 ± 14	67 ± 10	185 ± 36	21 ± 7
Na_2O-2.5SiO_2	79 ± 11	20 ± 6	-120 ± 6	30 ± 6	228 ± 41	48 ± 7
Na_2O-3SiO_2	84 ± 15	26 ± 5	-115 ± 22	30 ± 6	246 ± 47	61 ± 12

Figure 1: Cross section of the sample showing the analysed area.

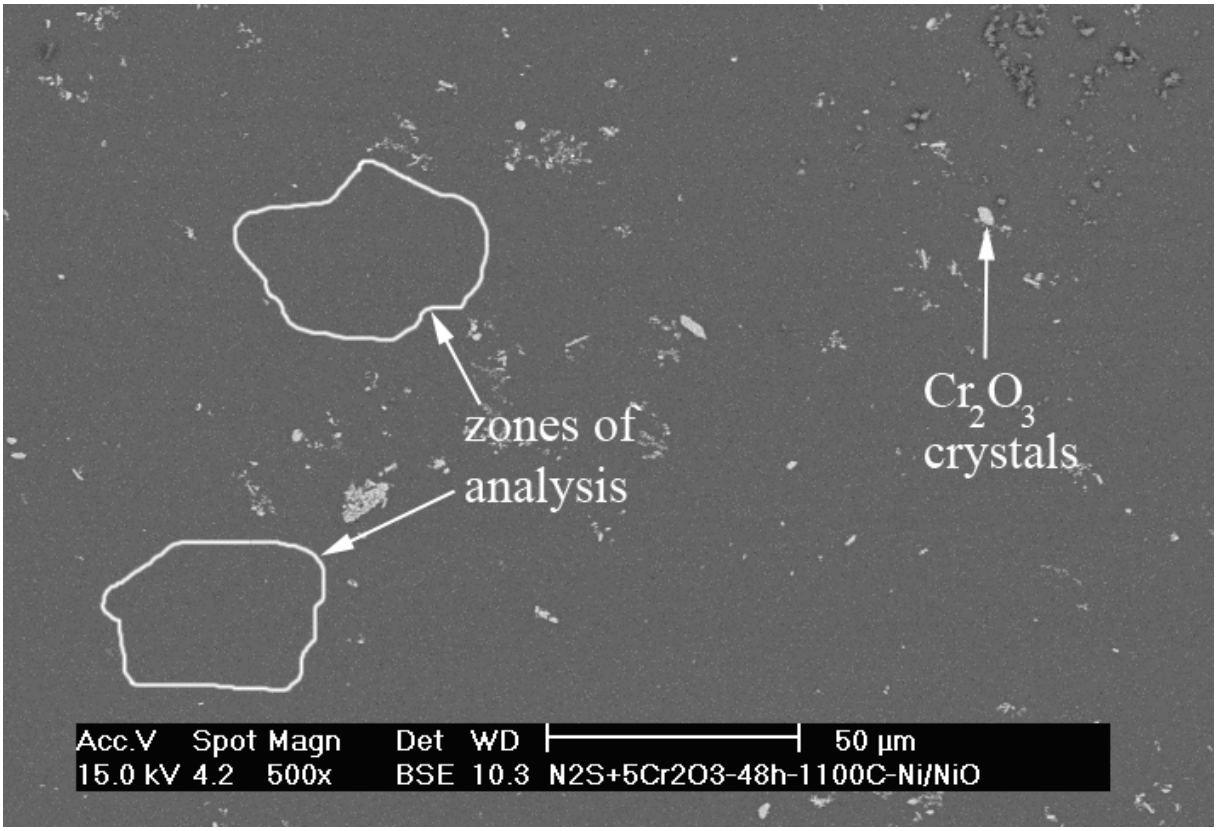

Figure 2: Total chromium contents reported as a function of oxygen fugacity for different temperatures and glass compositions. (a) T=1125°C – (b) T=1175°C – (c) T=1200°C – (d) T=1250°C.

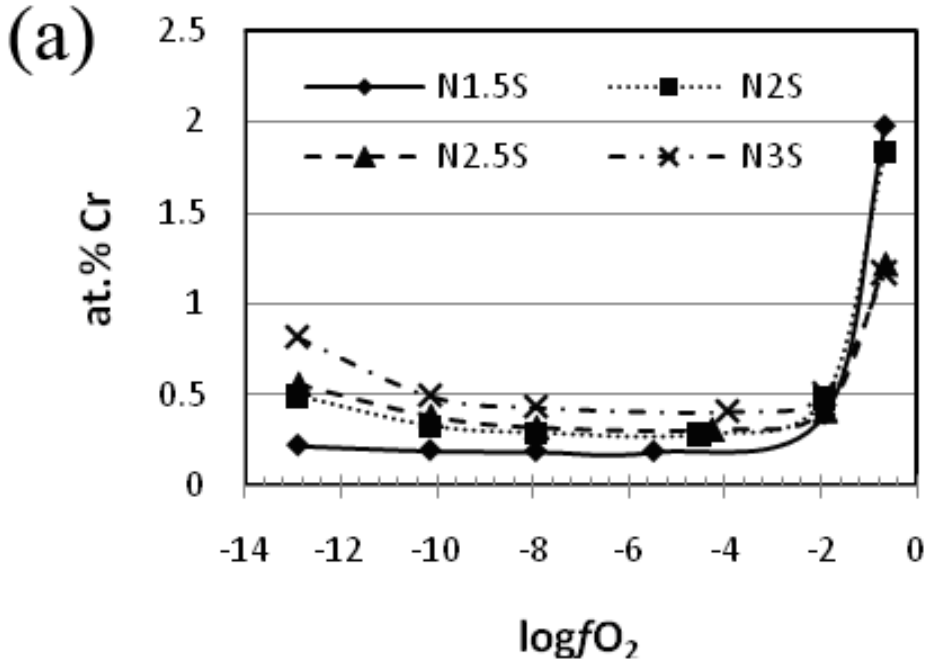

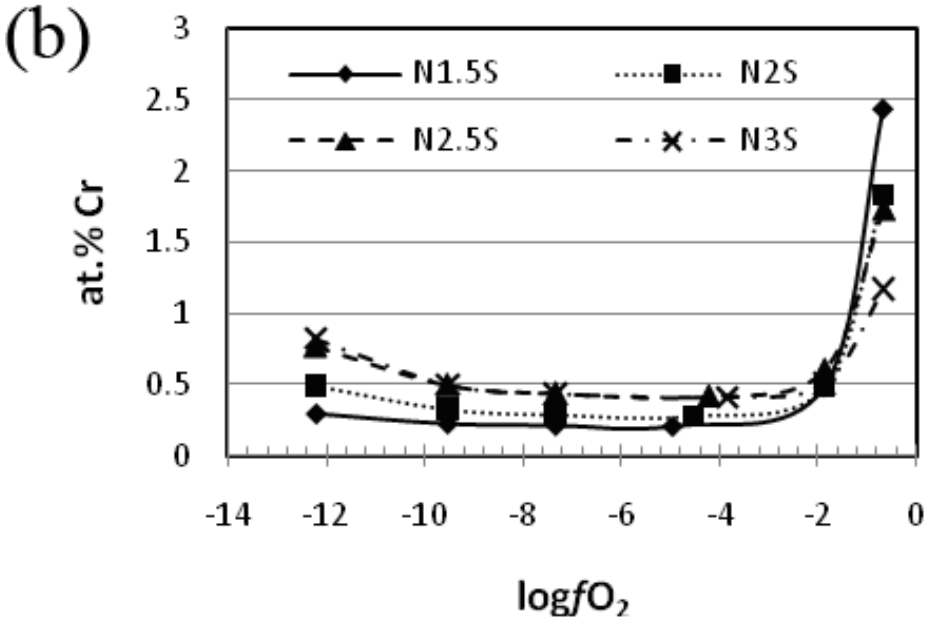

(c)

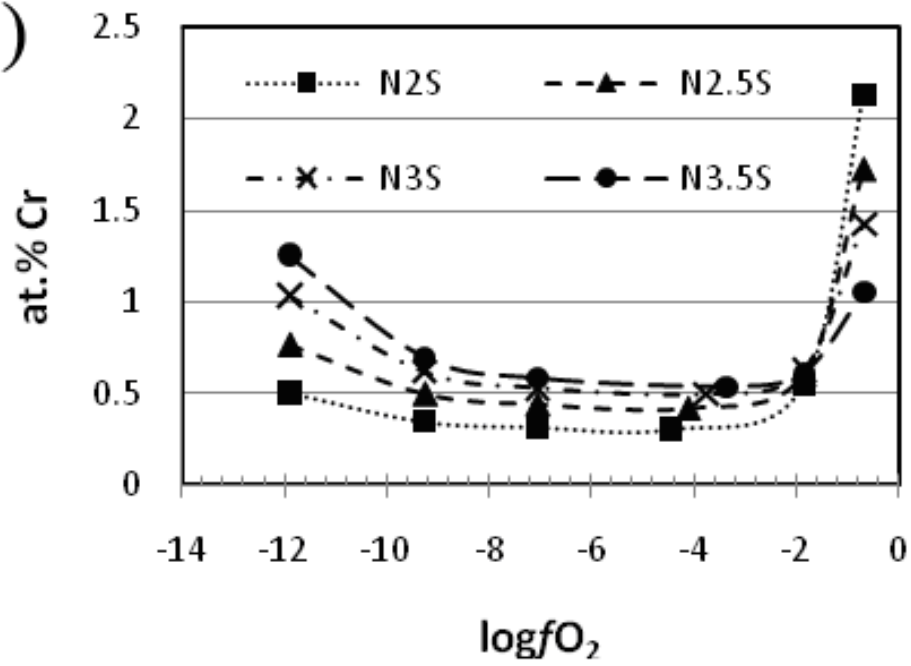
2.5
2
1.5
1
0.5
0
at.% Cr
N2S
N2.5S
N3S
N3.5S
-14
-12
-10
-8
-6
-4
-2
0
logfO_2

(d)

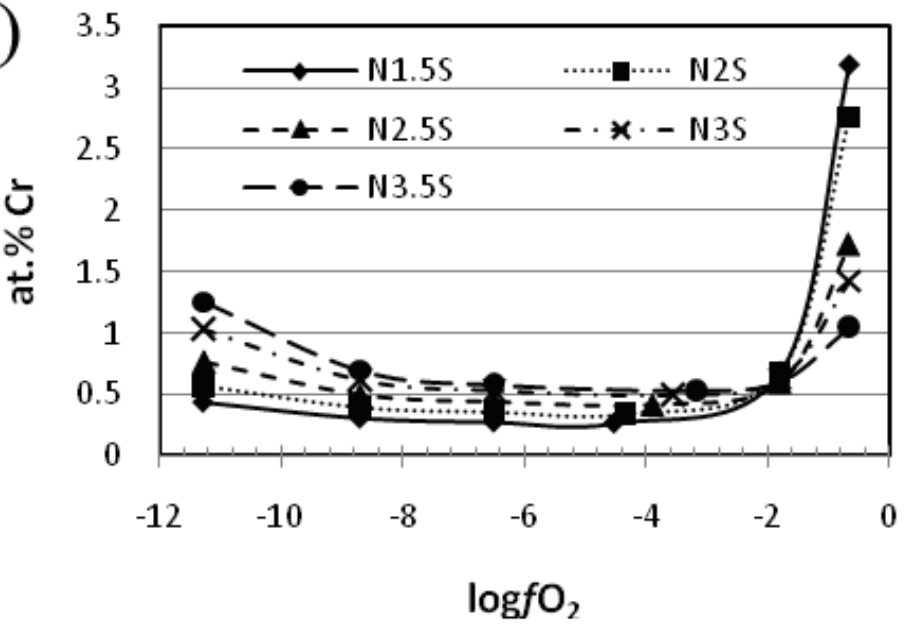
3.5
3
2.5
2
1.5
1
0.5
0
at.% Cr
N1.5S
N2S
N2.5S
N3S
N3.5S
-12
-10
-8
-6
-4
-2
0
logfO_2

Figure 3: Plots of total chromium contents in the Na_2O-$2SiO_2$ melt as a function of oxygen fugacity for different temperatures.

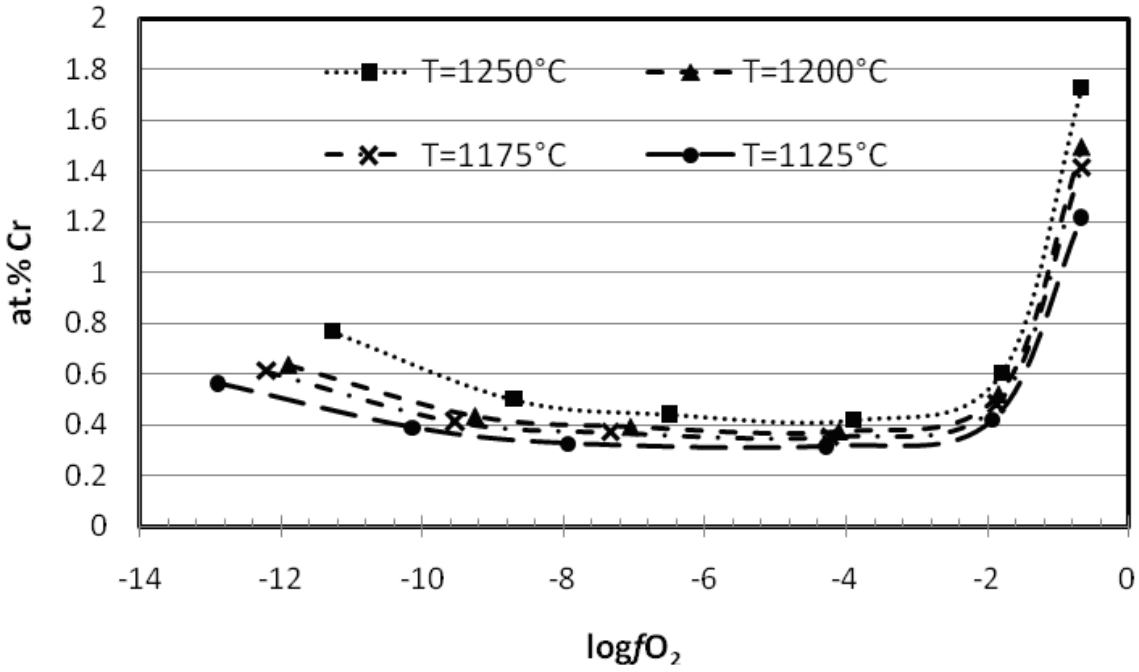

Figure 4: Plots of log(R_{red}) (a) and log(R_{ox}) (b) determined in the Na_2O-$2SiO_2$ system as a function of logfO_2 for different temperatures. The obtained equations of the lines are in agreement with the theoretical equations: **$\log(R_{red}) = -0.25\log(fO_2) + C$** and **$\log(R_{ox}) = 0.75\log(fO_2) + B$.** The values of B and C parameters deduced from these plots at each temperature are reported on the figure.

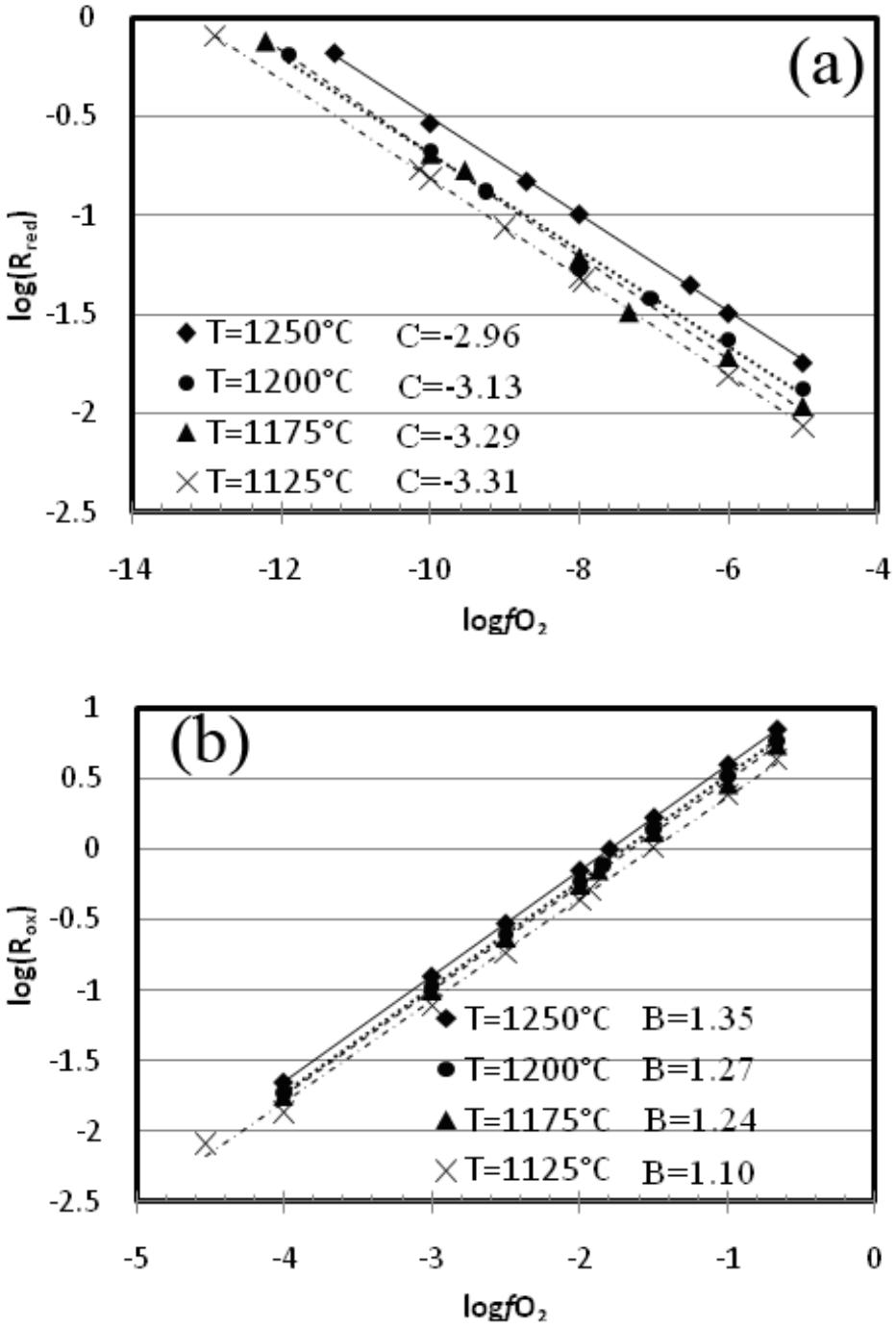

Figure 5: Logarithmic plot of Cr(III) (a), R_{ox} (b) and R_{red} (c) as a function of aO^{2-}.

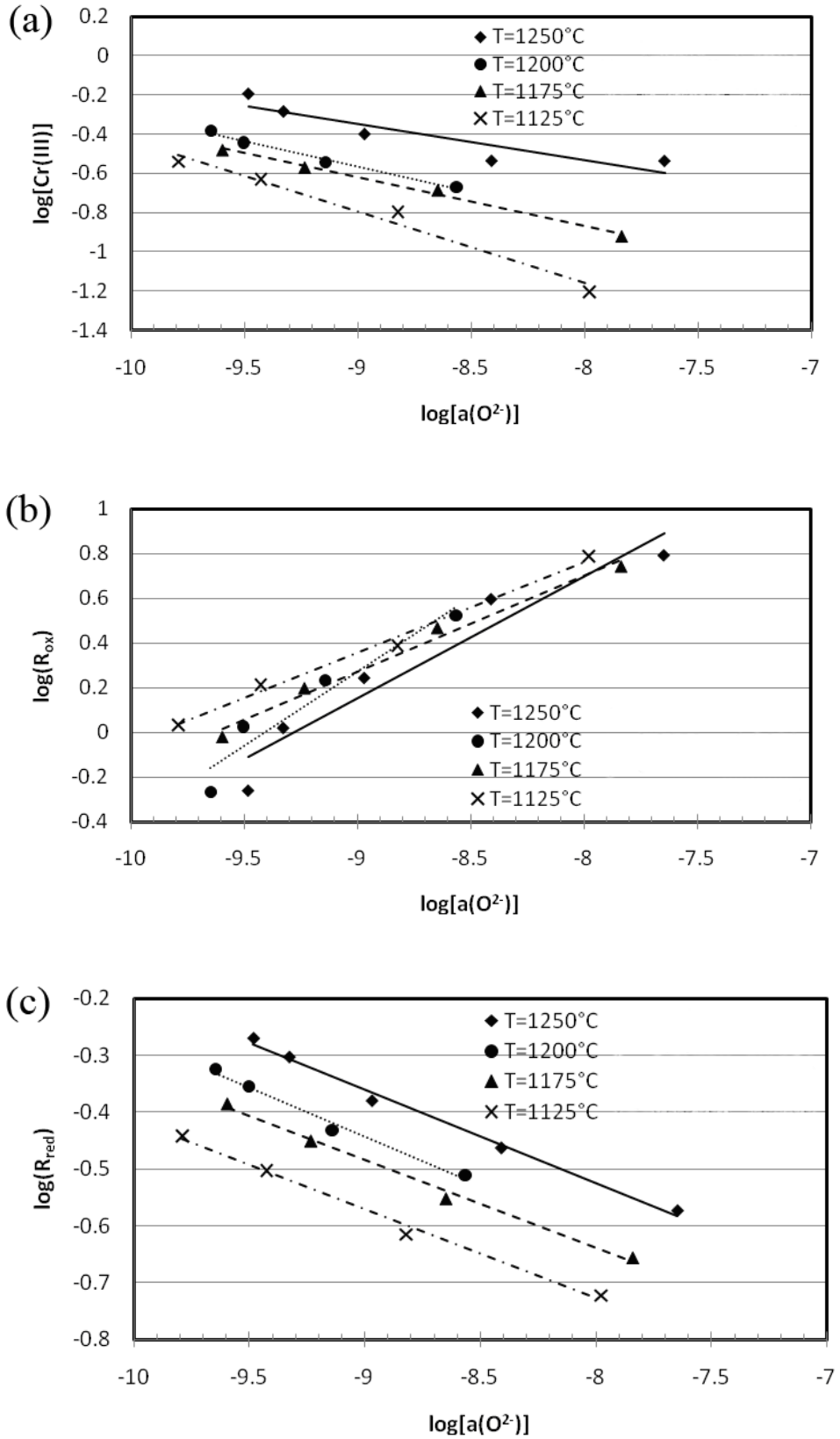

Figure 6: Stoichiometric coefficients x, y and z of the chromium oxo-complexes as a function of temperature.

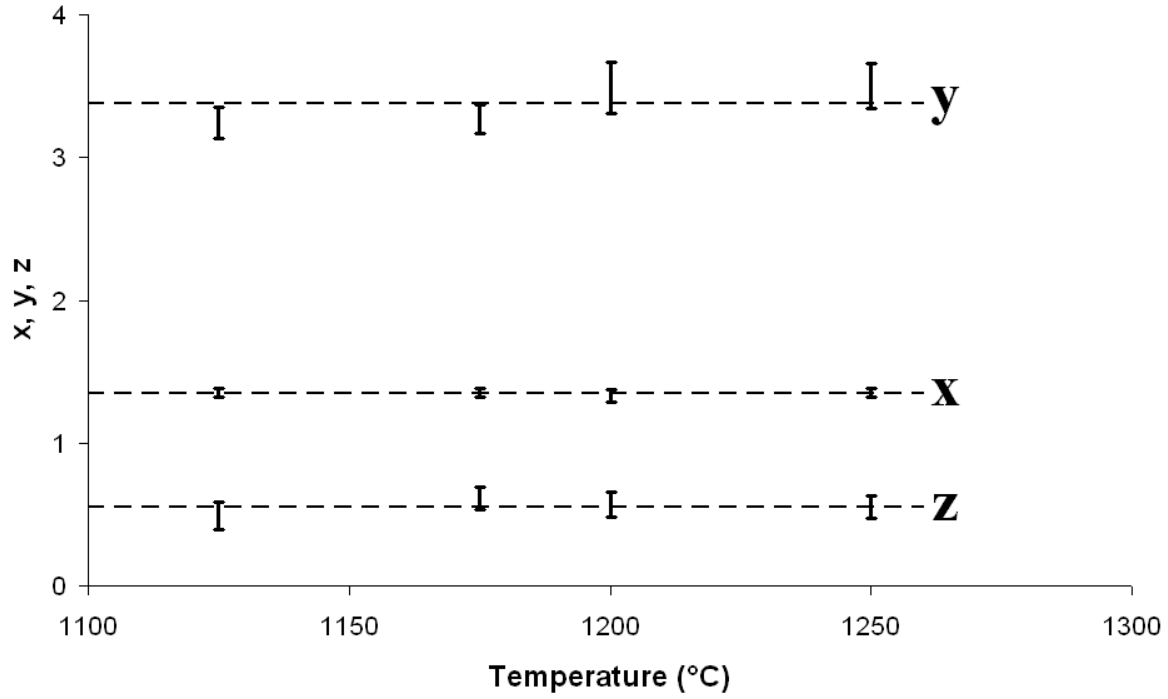

Figure 7: log[Cr(III)] reported as a function of 1/T for 4 compositions of the Na_2O-SiO_2 system:

Na_2O-1.5SiO_2: -0.252x+1.085 (R^2=0.999)

Na_2O-2SiO_2: -0.262x+1.262 (R^2=0.994)

Na_2O-2.5SiO_2: -0.212x+1.013 (R^2=0.996)

Na_2O-3SiO_2: -0.237x+1.258 (R^2=0.996)

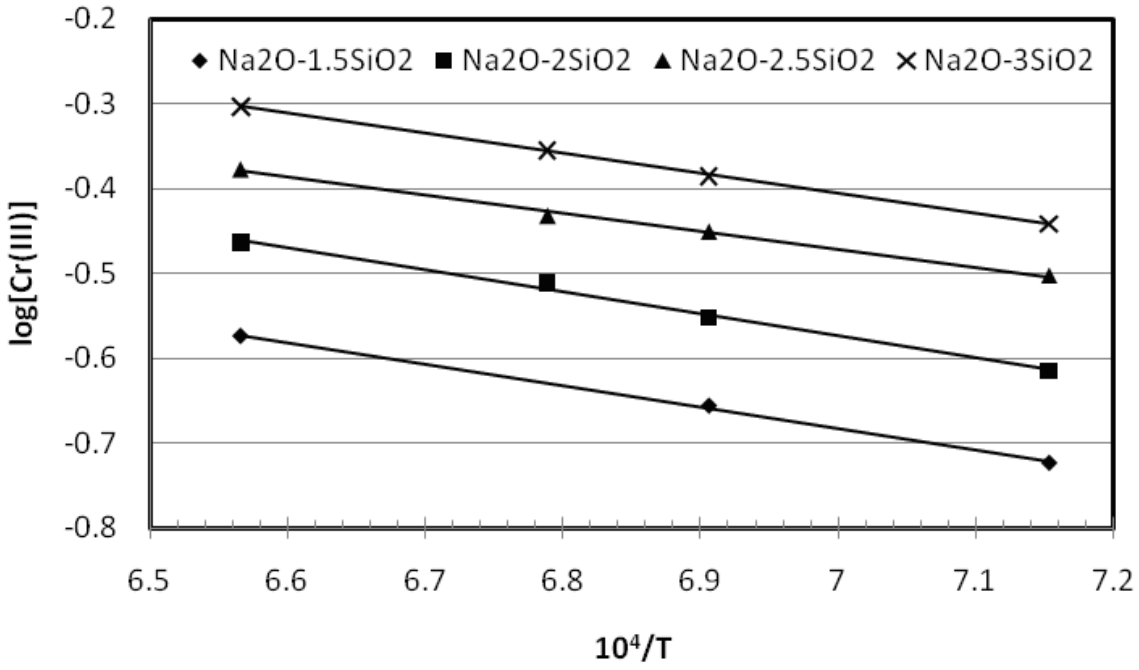

Figure 8: Plot of the B and C parameters as a function of the reverse of temperature. The results concern the Na_2O-$2SiO_2$ compositions